Capture of negative muons and antiprotons by noble-gas atoms

James S. Cohen*
Theoretical Division, Los Alamos National Laboratory, Los Alamos, New Mexico 87545
(Received 21 January 2002; published 3 May 2002)

Cross sections for capture of negative muons (μ^-) and antiprotons ($\bar{p}$) by helium, neon, argon, krypton, and xenon atoms are calculated using the fermion molecular dynamics method. These cross sections are used to estimate the capture ratios in mixtures.

DOI: 10.1103/PhysRevA.65.052714 PACS number(s): 36.10.−k, 34.10.+x, 25.43.+t, 03.65.Sq

I. INTRODUCTION

Capture of negative exotic particles (μ^-, π^-, K^-, and $\bar{p}$) by pure and mixed noble-gas atoms has long been of interest for observing the spectral and collisional properties of exotic atoms. These systems are free of behaviors that complicate the capture process in solid matter [1–3]. The present work uses a consistent theoretical approach—fermion molecular dynamics (FMD)—to determine the capture properties of He, Ne, Ar, Kr, and Xe, which are chemically similar but have widely varying numbers of electrons. Thus they provide a good set to see how the more tightly bound electrons affect the capture process. This extends the previous study of capture in He-Ne mixtures [4].

The present calculations have two principal goals: (i) to get an indication of the importance of correlation, so that requirements of a future quantum-mechanical method can be gauged and (ii) to determine, with useful accuracy, the kinetic energies at which the exotic particles are captured and the capture ratios in mixtures. Dynamical correlation in multielectron targets is much more difficult to treat quantum mechanically than in the present quasiclassical method. The best available comparison with experiments is the capture ratios, which have been measured, directly or indirectly, in mixtures of noble-gas atoms for muons and pions. These ratios are also of current interest for antiproton capture, but have not yet been determined experimentally with antiprotons.

The previous theoretical treatments of exotic negative particle capture by high-Z atoms used the Fermi-Teller method [5,6]. The Fermi-Teller method utilizes the Thomas-Fermi model for the target. This description does not provide an electronic shell structure or allow for correlation. The result was a Z-scaling law, and its variants, which experiments have shown to be too simplistic [7–9,2]. The FMD method includes correlation and yields a shell structure, though the shells obtained are generally not faithful to the real atoms.

II. THEORETICAL METHOD

A. Fermion molecular dynamics

The FMD method [10] utilizes the Kirschbaum-Wilets (KW) ansatz for atomic structure [11]. In this model, pseudopotentials V_H and V_P constrain the quasiclassical dynamics to satisfy the Heisenberg uncertainty and Pauli's exclusion principles, respectively. The resulting multielectron atom, which does not exist classically, is stabilized and possesses a shell structure [12]. Similar terms are included for the exotic atom structure, but have little effect since it is formed in highly excited states, which behave nearly classically according to the correspondence principle.

The FMD effective Hamiltonian for the system is written as

$$H_{\mathrm{FMD}} = H_0 + V_H + V_P , \tag{1}$$

where H_0 is the usual Hamiltonian of the system containing the kinetic energies of all particles and the Coulomb potentials for all pairs of particles. The extra terms are of the form

$$V_H = \sum_{i=1}^{N_e} f(r_{ni}, p_{ni}; \xi_H, \alpha_H) + f(r_{nx}, p_{nx}; \xi_H, \alpha_H) \tag{2}$$

and

$$V_P = \sum_{i=1}^{N_e} \sum_{j=i+1}^{N_e} f(r_{ij}, p_{ij}; \xi_P, \alpha_P)\, \delta_{s_i, s_j}, \tag{3}$$

where the sums are over the N_e electrons, r_{ni} (p_{ni}) is the relative distance (momentum) of electron i with respect to the nucleus n, r_{nx} (p_{nx}) is the relative distance (momentum) of the exotic particle x with respect to the nucleus n, r_{ij} (p_{ij}) is the relative distance (momentum) of electron j with respect to electron i, and s_i (s_j) is the spin of electron i (j). Hamilton's classical equations of motion are solved with the Hamiltonian H_{FMD}.

The constraining potentials are embodied by [11]

$$f(r_{\lambda\nu}, p_{\lambda\nu}; \xi, \alpha) = \frac{(\xi\hbar)^2}{4\alpha r_{\lambda\nu}^2 \mu_{\lambda\nu}} \exp\left\{ \alpha \left[1 - \left(\frac{r_{\lambda\nu} p_{\lambda\nu}}{\xi\hbar} \right)^4 \right] \right\} \tag{4}$$

where the subscripts λ and ν designate pairs of particles with reduced mass $\mu_{\lambda\nu}$. The parameter ξ reflects the size of the core (Heisenberg or Pauli) while α is the hardness parameter. The only way by which we deviate from the original prescription of KW is to use values of ξ_H and ξ_P optimized for the target atom, rather than the universal values [12], and softer values of α_H and α_P as recommended by Beck and Wilets [13]. The modification of the hardness parameters α_H and α_P is not as important for the low-energy collisions under present consideration as it was for the stopping powers

*Electronic address: cohen@lanl.gov

TABLE I. Optimized FMD parameters. The associated first ionization potentials and total energies are compared with accurate values (experimental for the ionization potential and Hartree-Fock (HF) for the total energy). In all cases, $\alpha_H=2.0$ and $\alpha_P=1.0$.

	FMD parameters		Associated energies (a.u.)			
	ξ_H	ξ_P	$IP_1^{(FMD)}$	$IP_1^{(expt)}$	$E_{tot}^{(FMD)}$	$E_{tot}^{(HF)}$
He	0.93		0.974	0.904	−2.81	−2.86
Ne	1.13	1.51	0.792	0.792	−129.1	−128.5
Ar	1.19	1.59	0.584	0.579	−525.0	−526.8
Kr	1.21	1.64	0.385	0.515	−2805.1	−2752.1
Xe	1.23	1.68	0.510	0.446	−7252.5	−7232.2

calculated by Beck and Wilets, but still we use the same values of $\alpha_H=2.0$ and $\alpha_P=1.0$.

The values of ξ_H and ξ_P were determined by nonlinear least-squares fits of H_{FMD} to match the experimental first ionization potential (IP_1) [14] and nonrelativistic Hartree-Fock total binding energy (E_{tot}) [15] of the target atom. This procedure is appropriate since the first ionization potential is expected to be most important for the capture dynamics and the higher ionization potentials will be correct on the average if the total energy is accurate. Near-exact fits were found for Ne, Ar, and Xe. This procedure is inherently approximate for He since its two electrons have antiparallel spins and thus the parameter ξ_P has no effect (α_H and α_P are not useful variables for this procedure). The best fit found for Kr was also somewhat inaccurate. The parameters obtained for the noble-gas atoms are given in Table I.

The optimized parameters significantly improve the FMD representation of the noble-gas atoms. The outer electrons reside in a closed shell and appear to have locally maximal ionization potentials (the adjacent elements were not actually calculated), which was not the case with the universal parameters [12]. For all the heavier noble-gas atoms, Ne-Xe, there are outermost quasishells of six electrons, with orbital energies that, though not identical, are substantially smaller than the other (core) electrons. There is no proof that these parameters are unique, but no other precise fits were found.

The present calculations treat all electrons explicitly. For the heaviest noble-gas atoms, this requires a lot of computer time. The $6(N_e+2)$ equations of motion, for the exotic particle, the nucleus, and the target electrons, are solved in the laboratory frame. The target nucleus is initially stationary at the origin, and the projectile is started at $x=-10a_0$ with impact parameter $y=b$ chosen by uniform sampling of $b^2 \in [(b_{i-1})^2,(b_i)^2]$.[1] In the first range $[b_0,b_1]$, $b_0=0$ and b_1 is taken to be such that a few ranges of impact parameters will be required to converge the cross sections with $b_{i+1}=\sqrt{2}b_i$. The target is initially orientated by a random Euler rotation.

The integration is checked every 2000 steps to see if the final state can be reliably identified. The possible results are capture (always accompanied by ionization), ionization without capture, excitation, or elastic scattering. Ionization is expected to be the predominant part of the slowing-down cross section, but inelastic and elastic collisions also contribute. However, only the ionization cross sections were converged. This limitation was imposed, in part, because nonionizing trajectories require longer integration times and larger impact parameters, but more important, because the quasiclassical method is not considered to be dependable for such scattering. Thus the calculated slowing-down cross sections should be considered to be lower bounds. For collisions with He, Ne, and Ar, both the capture and total ionization cross sections were converged. For Kr and Xe, only the capture cross section was converged, so slowing down is not determined even in this approximation.

In the ith range of impact parameter, the contribution to the cross section for a reaction R is given by

$$\sigma_R^{(i)}=\frac{N_i^{(R)}}{N_i^{\mathrm{tot}}}\pi[(b_i)^2-(b_{i-1})^2], \tag{5}$$

with standard statistical error (assuming a binomial distribution) [16]

$$\Delta\sigma_R^{(i)}=\sigma_R^{(i)}\left(\frac{N_i^{\mathrm{tot}}-N_i^{(R)}}{N_i^{\mathrm{tot}}N_i^{(R)}}\right)^{1/2}, \tag{6}$$

where $N_i^{(R)}$ is the number of trajectories in which R occurred out of the total N_i^{tot} trajectories run with $b\in[b_{i-1},b_i]$. The integrated cross section is thus

$$\sigma_R=\sum_i \sigma_R^{(i)}, \tag{7}$$

with estimated error

$$\Delta\sigma_R=\left(\sum_i (\Delta\sigma_R^{(i)})^2\right)^{1/2}. \tag{8}$$

Typically, the total number of trajectories run was ~2000 for He, ~300 for Ne, ~150 for Ar, ~100 for Kr, and ~50 for Xe targets. The limited number of trajectories run result in substantial Monte Carlo errors. Beyond the statistical errors, the main uncertainties come from the use of quasiclassical dynamics and the approximate target shell structure. Some indication of the accuracy of the FMD method can be gained from the FMD calculation of capture by the hydrogen atom [17], which is in remarkably good agreement with accurate quantum-mechanical calculations [18–22]. Quantum-mechanical calculations for multielectron targets would be far more challenging.

B. Capture in mixtures

The initial distribution of capture states is a result of the competition between slowing down and capture, which are functions of the collision energy. A rigorous formulation of

[1]Atomic units are used: distance (a_0) $=0.529\times10^{-8}$ cm, energy (a.u.) $=27.21$ eV.

TABLE II. Cross sections for capture of μ^- by noble-gas atoms.

	σ_{capt} (units of a_0^2)				
$E_{c.m.}$ (a.u.)	He	Ne	Ar	Kr	Xe
0.01	72.31±1.17	36.19±2.20			
0.10	18.98±0.28	12.82±0.51	42.98±2.07		
0.20	10.42±0.13	9.76±0.34	28.67±1.44		
0.30	7.59±0.12				
0.40	6.05±0.08	7.63±0.23	18.06±1.27		
0.50	5.13±0.07				
0.60	4.54±0.07	6.53±0.19	14.28±0.57		
0.70	4.12±0.07				
0.80	3.80±0.06	5.91±0.16	12.58±0.52		
0.90	3.59±0.06				
1.00	3.41±0.05	5.53±0.17	9.76±0.49	16.40±1.97	22.58±2.00
1.10	2.91±0.06				
1.20	2.02±0.07				
1.50	1.02±0.07	4.15±0.15	7.21±0.36		
2.00	0.59±0.05	3.46±0.10	5.51±0.41	8.48±1.83	11.78±2.15
2.50	0.33±0.04				
3.00	0.09±0.02	2.01±0.15	3.68±0.50	6.79±1.71	
4.00		1.63±0.05	2.26±0.47	4.27±0.84	7.85±2.15
6.00		0.86±0.03	1.70±0.43	3.96±1.39	5.89±2.01
8.00		0.49±0.04	1.27±0.38	2.07±0.21	2.83±0.77
10.00		0.35±0.04	0.85±0.32	1.45±0.22	2.51±0.28
12.00		0.22±0.04	0.99±0.35		
15.00		0.10±0.02	0.54±0.21		
18.00		0.03±0.01	0.27±0.15		
21.00		0.03±0.01	0.27±0.15		
25.00		0.01±0.01	0.09±0.06		
30.00			0.05±0.05		
35.00			0.04±0.02		
40.00			0.03±0.02		
45.00			0.01±0.01		

the capture distributions has been given in terms of the ''arrival function,'' $F_{arr}(E_{lab})$, which is the solution of the integral equation [23,24]

$$F_{arr}(E)=\int_0^\infty \Theta(E-\epsilon)\,\frac{1}{\sigma(E+\epsilon)}\,\frac{d\sigma(E+\epsilon,\epsilon)}{d\epsilon}F_{arr}(E+\epsilon)d\epsilon, \tag{9}$$

where $d\sigma(E,\epsilon)/d\epsilon$ is the cross section for energy loss ϵ in a collision with energy E, $\sigma(E)$ is the total energy-loss cross section, and Θ is the unit step function. In principle, the differential cross section is required at all energies, ranging from that of the fast ($\gg 1$ keV) free muon or antiproton down to near-zero energy since some particles are not captured until they are essentially stopped.

In the present work, cross sections have been calculated only at energies where capture is probable, and even at these energies, only the contribution of ionization, not elastic and inelastic scattering, to the slowing down has been taken into account. Calculations of μ^- capture by the hydrogen atom [24] suggested that the slowing-down and capture mechanisms are similar, with capture resulting when the energy loss (ionization potential of the target + kinetic energy of the ionized electron) exceeds the incident energy of the exotic particle. As long as the typical energy loss is comparable to or greater than the energies at which capture occurs, the arrival function $F_{arr}(E_{lab})$ can be expected to be fairly flat and the capture profile,

$$F_{capt}(E_{lab})=\frac{\sigma_{capt}(E_{lab})}{\sigma_{tot}(E_{lab})}F_{arr}(E_{lab}), \tag{10}$$

can be adequately determined by just the ratio of the capture-to-total cross sections to within a normalization constant. Then the probability that the particle is captured before it is slowed to energy E_{lab} is given by

$$P_{capt}(E_{lab})\approx N\int_{E_{lab}}^\infty \frac{\sigma_{capt}(E'_{lab})}{\sigma_{tot}(E'_{lab})}dE'_{lab}, \tag{11}$$

where N is such that $P_{capt}(0)=1$.

TABLE III. Cross sections for capture of $\overline{p}$ by noble-gas atoms.

	σ_{capt} (units of a_0^2)				
$E_{\text{c.m.}}$ (a.u.)	He	Ne	Ar	Kr	Xe
0.01	77.76±1.13	32.23±1.98			
0.10	18.20±0.28	13.82±0.41	46.94±1.91		
0.20	9.55±0.14	10.04±0.35	30.24±1.40		
0.30	6.90±0.09				
0.40	5.34±0.06	7.99±0.24	17.67±0.83		
0.50	4.56±0.07				
0.60	3.94±0.06	6.41±0.14	13.85±0.40		
0.70	3.54±0.05				
0.80	3.27±0.05	6.38±0.17	10.46±0.50		
0.90	3.05±0.05				
1.00	2.91±0.05	5.66±0.13	8.77±0.43	15.55±3.14	19.64±1.35
1.10	1.76±0.07				
1.20	0.95±0.06				
1.50	0.38±0.05	3.71±0.12	5.94±0.37		
2.00	0.10±0.03	2.61±0.12	4.38±0.49	7.35±1.75	11.78±2.15
2.50	0.01±0.01				
3.00		1.66±0.16	2.69±0.49	6.22±1.66	
4.00		1.19±0.15	2.12±0.46	3.52±0.80	6.87±2.09
6.00		0.66±0.13	1.55±0.41	2.75±0.96	4.40±1.34
8.00		0.41±0.11	0.99±0.35	1.70±0.22	2.83±0.77
10.00		0.22±0.08	0.56±0.27	1.19±0.22	1.88±0.34
12.00		0.03±0.03	0.71±0.30		
15.00			0.27±0.15		
18.00			0.27±0.15		
21.00			0.18±0.12		
25.00			0.09±0.06		
30.00			0.02±0.02		
35.00			0.02±0.01		

In a binary mixture, assuming a flat arrival function, the probability of capture by component i is given by

$$W_i \approx N \int_0^\infty \frac{c_i \sigma_{\text{capt}}^{(i)}(E_{\text{lab}})}{c_1 \sigma_{\text{tot}}^{(1)}(E_{\text{lab}}) + c_2 \sigma_{\text{tot}}^{(2)}(E_{\text{lab}})} dE_{\text{lab}}, \qquad (12)$$

where c_1 and c_2 are the fractions of each species, $c_1+c_2=1$, and N is a normalization constant such that $W_1+W_2=1$. Here it is important that the cross sections for different species should be for the same lab (μ^- or $\overline{p}$) kinetic energy. The generalization to a mixture with more than two components is straightforward.

The most informative way of looking at capture is via the reduced capture ratio, i.e., the ratio of capture probabilities *per atom*,

$$A(Z_1,Z_2) = \frac{W_1/c_1}{W_2/c_2}. \qquad (13)$$

Note that, with this definition, $A(Z_2,Z_1)=1/A(Z_1,Z_2)$. If the process is linear, then this ratio is independent of c_1 and c_2; however, as first pointed out by Vogel *et al.* [25], the reduced capture ratio can, in fact, depend on the concentration.

III. RESULTS

The results for negative muon and antiproton capture by the noble-gas atoms are given in Tables II and III, respectively, as a function of center-of-mass (c.m.) system energy. The results for He and Ne were previously published [4]. The capture cross sections extend to collision energies well over 100 eV for all the atoms except He. For helium, the capture cross section decreases rapidly at collision energies exceeding its first ionization potential; this behavior is similar to that of the hydrogen atom and can be interpreted as quasiadiabatic ionization (strictly adiabatic ionization of helium cannot occur since the united-atom limit, H^-, is bound). On the other hand, the capture cross sections for the heavier atoms display no obvious alteration in behavior at collision energies equal to their ionization energies, which is the maximum collision energy at which ionization of a single electron, carrying off zero kinetic energy, suffices to capture the incident exotic particle. We believe this smoothness is due to

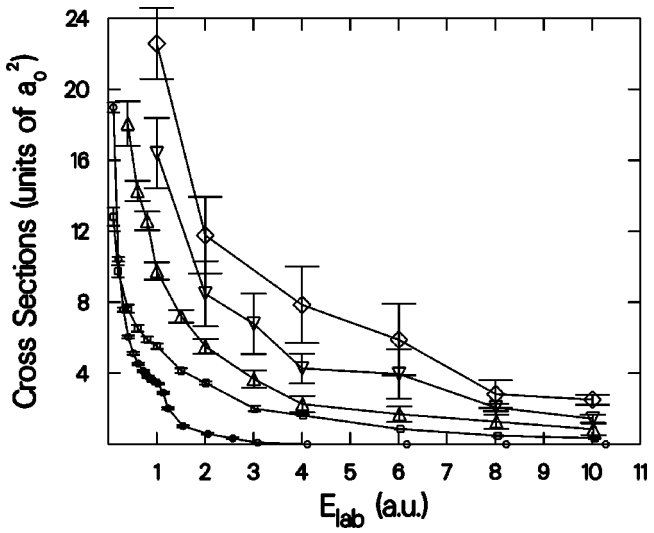

FIG. 1. Cross sections for negative muon capture by He (circle), Ne (square), Ar (up triangle), Kr (down triangle), and Xe (diamond) as a function of incident muon energy, with Monte Carlo error bars of the FMD calculation.

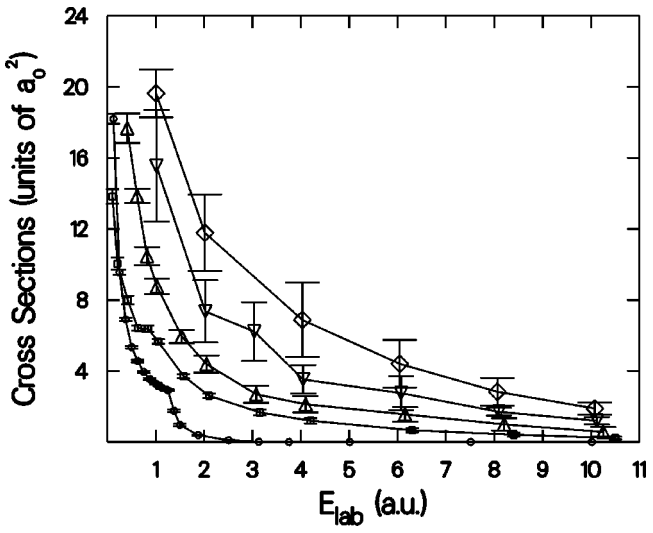

FIG. 2. Cross sections for antiproton capture by He (circle), Ne (square), Ar (up triangle), Kr (down triangle), and Xe (diamond) as a function of incident antiproton energy, with Monte Carlo error bars of the FMD calculation.

the fact that electron correlation in the heavier atoms is more intricate, and it is easier to excite or ionize additional electrons. Except for He and Ne at very low collision energies, the capture cross sections at a given energy increase monotonically with the Z of the noble gas.

The capture cross sections for $\bar{p}$ are very similar to those for μ^-. In the c.m. system, the μ^- cross sections tend to be slightly larger than the $\bar{p}$ cross sections. This can be attributed to the fact that nonadiabatic effects are larger for the lighter particle. The cross sections are shown as a function of laboratory energy, which is more relevant to capture in mixtures, in Figs. 1 and 2. The difference between the c.m. system and laboratory system energies is appreciable only for the $\bar{p}+\mathrm{He}$ collision; in the laboratory system, the $\bar{p}+\mathrm{He}$ cross section is actually larger than the $\mu^-+\mathrm{He}$ cross section in a narrow, but statistically significant, energy region just above $E_{\mathrm{lab}}=1$ a.u.

The reduced capture ratios are calculated by Eqs. (12) and (13). As mentioned above, the total slowing-down cross sections that appear in Eq. (12) have not been calculated. However, the behaviors found in the total ionization cross sections, calculated for He, Ne, and Ar, suggest a reasonable approximation. We first observe that an ionizing collision at c.m. system collision energy below the first target ionization potential (IP) must, by energy conservation, result in capture. The total ionization cross sections, calculated by FMD for He, Ne, and Ar targets, are found to decrease relatively slowly at higher collision energies within the range of capture energies ($\lesssim 10$ a.u.). As an approximation, we thus take

$$\sigma_{\mathrm{ion}}(E)\approx\begin{cases}\sigma_{\mathrm{capt}}(E) & \text{at } E\leqslant 1.0 \text{ a.u.}\\ \sigma_{\mathrm{capt}}(1.0 \text{ a.u.}) & \text{at } E>1.0 \text{ a.u.}\end{cases} \tag{14}$$

We make the further approximation

$$\sigma_{\mathrm{tot}}(E)\approx\sigma_{\mathrm{ion}}(E). \tag{15}$$

Really σ_{ion} is a lower bound on σ_{tot}, but any shortfall may be compensated by the approximation in Eq. (14), which

TABLE IV. Capture ratios for negative muons (and pions) in equimolar binary mixtures.

		Experiments						
	Theory	Ref. [27]	Ref. [28]	Ref. [29]	Ref. [30]	Ref. [31]	Ref. [32]	Ref. [33]
A(Ne,He)	3.3		4.1		3.4	5.5	4.2	
A(Ar,He)	7.6		6.8		4.8	6.1	6.4	
A(Kr,He)	9.7				6.4	11.	9.1	
A(Xe,He)	13.9					12.	11.	
A(Ar,Ne)	2.2	1.1	1.6	1.1	1.4	1.1	1.5	1.26
A(Kr,Ne)	2.9	2.3			1.9	1.9	2.1	
A(Xe,Ne)	4.3	2.3				2.1	2.7	
A(Kr,Ar)	1.4	2.2			1.3	1.8	1.4	
A(Xe,Ar)	2.0	2.2				1.9	1.8	
A(Xe,Kr)	1.4	1.0				1.1	1.2	

TABLE V. Capture ratios for antiprotons in equimolar binary mixtures.

	Theory
A(Ne,He)	3.0
A(Ar,He)	7.0
A(Kr,He)	8.7
A(Xe,He)	12.8
A(Ar,Ne)	2.2
A(Kr,Ne)	3.0
A(Xe,Ne)	4.4
A(Kr,Ar)	1.4
A(Xe,Ar)	2.1
A(Xe,Kr)	1.5

generally somewhat exceeds the actual ionization contribution at the higher energies. The sensitivity to these approximations is examined below.

The resulting capture ratios for equimolar binary mixtures are given in Tables IV and V for μ^- and $\bar{p}$, respectively. The capture fractions increase monotonically with Z, though not proportional to some power of Z or with any other simple Z dependence. The values for μ^- capture (or π^- initial capture, which is almost the same) are similar to the experimental values; they are generally a bit higher except for A(Ne,He). The lower value for A(Ne,He) reflects the anomalous crossing of the neon and helium cross sections at low energies; possibly the experimental values indicate that this crossing is spurious.

As expected from the similarity of their capture cross sections, the ratios for $\bar{p}$ capture differ from those of μ^- only slightly. As yet, there are no experimental values available for $\bar{p}$ capture in the mixtures.

Most of the experimental determinations are indirect; i.e., the ratios are really quotients or products of ratios with some species in common, e.g.,

$$A(Z_1,Z_2)=A(Z_1,Z_3)A(Z_3,Z_2). \tag{16}$$

TABLE VI. Comparison of indirectly calculated with directly calculated capture ratios for negative muons in equimolar mixtures. An extra digit is given to facilitate the comparison.

		Indirect	
	Direct	With Ar	With ^{3}He
A(Ne,He)	3.29	3.52	3.29
A(Ar,He)	7.59	7.59	7.58
A(Kr,He)	9.67	10.34	9.67
A(Xe,He)	13.89	14.95	13.90
A(Ar,Ne)	2.15	2.15	2.31
A(Kr,Ne)	2.94	2.93	2.94
A(Xe,Ne)	4.26	4.24	4.23
A(Kr,Ar)	1.36	1.36	1.28
A(Xe,Ar)	1.97	1.97	1.83
A(Xe,Kr)	1.45	1.45	1.44

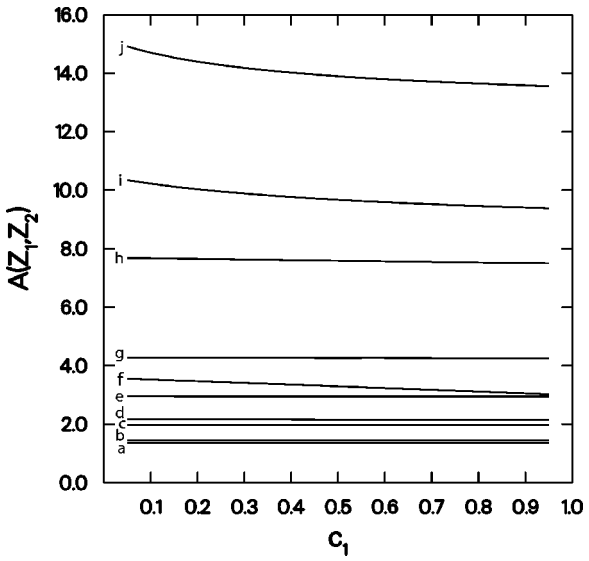

FIG. 3. Calculated concentration dependences for capture of muons in binary mixtures of noble-gas atoms. From bottom to top, the curves are (a) A(Kr,Ar), (b) A(Xe,Kr), (c) A(Xe,Ar), (d) A(Ar,Ne), (e) A(Kr,Ne), (f) A(Ne,He), (g) A(Xe,Ne), (h) A(Ar,He), (i) A(Kr,He), and (j) A(Xe,He).

We have the data to test this hypothesis with Ar and ^{3}He as the common element. It can be seen in Table VI that Eq. (16) appears to be a good approximation, off by $\sim$10% in the worst of these cases.

Next we examine the sensitivity to the assumption of Eqs. (14) and (15). Determinations with the actual FMD ionization cross sections for He, Ne, and Ar [instead of Eqs. (14) and (15)] yield A(Ne,He)=3.7, A(Ar,He)=9.5, and A(Ar,Ne)=2.3 for μ^-, and A(Ne,He)=3.4, A(Ar,He) =9.9, and A(Ar,Ne)=2.3 for $\bar{p}$, in reasonable agreement with Tables IV and V.

The mixtures with helium are moderately sensitive to the slowing-down cross sections: a factor of 2 increase in $\sigma_{\rm tot}$ decreased the capture ratios by up to 20% and a factor of 2 decrease in $\sigma_{\rm tot}$ increased the capture ratios by up to 50%. All the capture ratios for mixtures without helium are quite insensitive to the slowing-down cross sections: a factor of 2 change in $\sigma_{\rm tot}$ changed the capture ratios by no more than 2% for μ^- and 5% for $\bar{p}$. The reason for the greater sensitivity with helium is its much sharper energy cutoff in capture.

Figure 3 shows the dependences of the reduced capture ratios [Eq. (13)] on the concentration c_1 of the heavier component. The concentration dependences are found to be rather weak, so comparison of measurements utilizing different concentrations, as done in Table IV, is legitimate. The strongest dependence is seen in the mixtures with helium, especially at small concentrations of the heavier element. This is because the significantly larger slowing-down cross section of the heavier element enables more muons to reach energies below the cutoff in the helium capture cross section.

IV. CONCLUSIONS

Negative muon and antiproton capture cross sections have been calculated by the FMD method for all noble-gas targets.

The all-electron calculations for the heaviest atoms are quite time consuming and might benefit from the use of a core potential to eliminate the inner shells. However, the increase in the cross sections even for the heaviest atoms, for which the ionization potentials are similar, suggests that correlation is important, so the elimination of electrons must be done with care.

Although the quasiclassical method may overestimate correlation, it seems clear that multiple electrons participate in the capture and any one-electron method is destined to fail. For example, a recent theoretical treatment with a single active electron by Briggs *et al.* [26] obtained cross sections for $\bar{p}$ capture by helium, neon, and argon. Their results are not too different from the present results for helium, but decrease instead of increasing for neon and argon. The corresponding capture ratios are $A(\mathrm{Ne,He})\approx 0.04$, $A(\mathrm{Ar,He})\approx 0.004$, and $A(\mathrm{Ar,Ne})\approx 0.01$. Since even this one-electron method indicates that μ^- and $\bar{p}$ capture are similar, these results appear to be in drastic disagreement with experiments. A multielectron quantum-mechanical calculation is highly desirable; time-dependent methods, as previously used for capture of muons and antiprotons by the hydrogen atom [18,21,22], may soon be up to the task.

The relative capture probabilities for the noble-gas atoms increase with Z due to the higher-Z capture cross sections being larger at a given energy as well as extending to higher collision energies. Except for changes in magnitude, Ne, Ar, Kr, and Xe behave in a qualitatively similar fashion, but He is different. The He capture cross section decreases abruptly at collision energies exceeding its first ionization potential, rather like capture by the hydrogen atom [17], but the capture cross sections of the heavier noble gases are smooth at this juncture.

The present calculations of capture ratios are somewhat inadequate because the corresponding slowing-down cross sections have not been completely determined—elastic and nonionizing inelastic contributions have not been calculated, nor have the noncapture ionization cross sections been calculated for Kr and Xe. In their place, the total slowing-down cross section has been approximated by the capture cross section at $E_{\mathrm{c.m.}}\leqslant 1.0$ a.u. and continued to higher energies by its value at 1.0 a.u. The resulting capture ratios are in reasonable agreement with available experimental values. More work on slowing down is needed before it can be ascertained whether the remaining disagreements with experimental results are due to the slowing-down cross sections or to the capture cross sections themselves.

The often-used experimental procedure of estimating capture ratios by actually observing capture in separate mixtures with a third element in common was found to be a reasonably good approximation. Also, the capture ratios depend only weakly on the relative concentrations, so it is sensible to extrapolate capture ratios measured at convenient concentrations.

ACKNOWLEDGMENTS

I thank D. Horváth for helpful comments. This work was done under the auspices of the U.S. Department of Energy.

[1] T. von Egidy and F.J. Hartmann, Phys. Rev. A **26**, 2355 (1982).
[2] T. von Egidy, D.H. Jakubassa-Amundsen, and F.J. Hartmann, Phys. Rev. A **29**, 455 (1984).
[3] D. Horváth and F. Entezami, Nucl. Phys. A **407**, 297 (1983).
[4] J.S. Cohen, Phys. Rev. A **62**, 022512 (2000).
[5] E. Fermi and E. Teller, Phys. Rev. **72**, 399 (1947).
[6] M. Leon and R. Seki, Nucl. Phys. A **282**, 445 (1977).
[7] V.G. Zinov, A.D. Konin, and A.I. Mukhin, Yad. Fiz. **2**, 859 (1965) [Sov. J. Nucl. Phys. **2**, 613 (1966)].
[8] H. Schneuwly, V.I. Pokrovsky, and L.I. Ponomarev, Nucl. Phys. A **312**, 419 (1978).
[9] H. Daniel, W. Denk, F.J. Hartmann, W. Wilhelm, and T. von Egidy, Phys. Rev. Lett. **41**, 853 (1978).
[10] For a review, see L. Wilets and J.S. Cohen, Contemp. Phys. **39**, 163 (1998).
[11] C.L. Kirschbaum and L. Wilets, Phys. Rev. A **21**, 834 (1980).
[12] J.S. Cohen, Phys. Rev. A **51**, 266 (1995); **57**, 4964 (1998).
[13] W.A. Beck and L. Wilets, Phys. Rev. A **55**, 2821 (1997).
[14] W. Däppen, in *Allen's Astrophysical Quantities*, edited by A. N. Cox (AIP-Springer, New York, 2000), Chap. 3.
[15] C.F. Fischer, At. Data Nucl. Data Tables **12**, 87 (1973).
[16] R. Abrines and I.C. Percival, Proc. Phys. Soc. **88**, 861 (1966).
[17] J.S. Cohen, J. Phys. B **31**, L833 (1998).
[18] N.H. Kwong, J.D. Garcia, and J.S. Cohen, J. Phys. B **22**, L633 (1989).
[19] A. Boukour, R.N. Hewitt, and C. Leclercq-Willain, Hyperfine Interact. **101/102**, 263 (1996).
[20] K. Ohtsuki, Y. Ishida, M. Matsuzawa, and M. Shinada, in *Abstracts of the 21st International Conference on the Physics of Electronic and Atomic Collisions*, edited by Y. Itikawa *et al.*, (XXI ICPEAC, Tokyo, 1999), p. 438.
[21] K. Sakimoto, Phys. Rev. A **65**, 012706 (2002).
[22] K. Sakimoto, J. Phys. B **35**, 997 (2002).
[23] M. Leon, Phys. Rev. A **17**, 2112 (1978).
[24] J.S. Cohen, Phys. Rev. A **27**, 167 (1983).
[25] P. Vogel, P.K. Haff, V. Akylas, and A. Winther, Nucl. Phys. A **254**, 445 (1975).
[26] J.S. Briggs, P.T. Greenland, and E.A. Solov'ev, J. Phys. B **32**, 197 (1999).
[27] P. Ehrhart *et al.*, Phys. Rev. A **27**, 575 (1983); Z. Phys. A **311**, 311 (1983), average at different concentrations.
[28] Yu.G. Budysahov *et al.*, Phys. At. Nucl. Russian **5**, 830 (1967) [Sov. J. Nucl. Phys. **5**, 589 (1967)], with Ar in common.
[29] H.-J. Pfeiffer *et al.*, Nucl. Phys. A **254**, 433 (1975).
[30] R.L. Hudson *et al.*, Phys. Lett. **76A**, 226 (1980), with Ar in common.
[31] A.V. Bannikov *et al.*, Nucl. Phys. A **403**, 515 (1983), pions, with ^{3}He in common.
[32] V.I. Petrukhin and V.M. Suvorov, Zh. Eksp. Teor. Fiz. **70**, 1145 (1976) [Sov. Phys. JETP **43**, 595 (1976)], pions, with H_2 in common.
[33] Y.-A. Thalmann *et al.*, Z. Phys. A **359**, 219 (1997); Phys. Rev. A **57**, 1713 (1998).